

## Atomic data from the iron project.

### XIII. Electron excitation rates and emissivity ratios for forbidden transitions in Ni II and Fe II

M.A. Bautista and A.K. Pradhan

Dept. of Astronomy, Ohio State University, Columbus, Ohio 43210-1106, U.S.A.  
 Internet: bautista@payne.mps.ohio-state.edu pradhan@payne.mps.ohio-state.edu

Received May 29; accepted May 30, 1995

**Abstract.** — Electron impact excitation rates and emissivity line ratios are reported for Optical and IR transitions in Ni II and Fe II arising from low-lying even parity levels. A total of 7 LS terms were included for Ni II, which result in 17 fine structure levels and 136 transitions. Coupling effects and resonance structures considered in the present calculations result in significant differences with the earlier distorted wave calculations by Nussbaumer & Storey (1982), although a reasonable agreement is found for the line diagnostics of some strong transitions in Ni II. Whereas an extensive set of collisional data has been presented earlier by Zhang & Pradhan for Fe II in the Iron Project series, in this paper we report collision strengths for some transitions missing from their dataset using an improved eigenfunction expansion for Fe II which includes the lowest 18 LS terms giving 52 fine structure levels and 1326 transitions. The present dataset provides a useful check on several forbidden transitions in Fe II and essentially confirms the diagnostics derived from the earlier work. The present calculations were carried out on the massively parallel processor Cray T3D with a parallelized version of the Iron Project R-matrix codes; to our knowledge these are the first such calculations.

**Key words:** atomic data — infrared: general

#### 1. Introduction

Nickel is one of the iron peak elements whose lines have been identified in a large variety of astronomical objects, but use of these lines for plasma diagnostics and Nickel abundance estimations have so far led to uncertain and ambiguous results. Until now only one previous computation of electron impact excitation rates for Ni II has been reported (Nussbaumer & Storey 1982; hereafter NS), and when this data have been used to estimate the Nickel abundance it have led to abnormally high abundances of this element with respect to Iron in comparison with the cosmic value. This problem is known as the nickel-to-iron problem and is well known in the context of H II regions like the Orion nebula (e.g. Grandi 1975; Osterbrock et al. 1992), supernova remnants (e.g. Dennefeld & Péquignot 1983; Dennefeld 1986; Henry et al. 1984; Hugins et al. 1990; Rudy et al. 1994), and circumstellar nebulae of luminous blue variables (e.g. Stahl & Wolf 1986; Johnson et al. 1992). A compilation of apparent Ni/Fe ratios in a variety of sources is presented by Henry & Fesen (1988)

and they hypothesize that there might be large errors in the collisional data by NS. For this reason an accurate calculation of collision strengths and excitation rates for Ni II is of great interest.

Considerable amount of effort and resources have been dedicated recently to the computation of reliable collisional data for Fe II (Pradhan & Berrington 1993; Pradhan & Zhang 1993, hereafter PZ; Zhang & Pradhan 1995, hereafter ZP). These data have been used for diagnostics of astronomical plasmas since it began to become available, and have proven to be of great importance. As an example, [Fe II] line ratios have led to the discovery of high electron density, low ionization zones in the Orion nebula and other H II regions (Bautista et al. 1994; Bautista & Pradhan 1995a). It is important, then, to attempt to check on the accuracy of these collisional excitation rates and emissivity ratios. Also, while the earlier Fe II calculations included many of the quartet and sextet states, the doublets and some sextets were excluded. It is therefore desirable to obtain excitation rates for transitions among the doublets and sextets, for example corresponding to some important lines at  $\lambda 4287$ ,  $\lambda 7452$ , and

---

Send offprint requests to: M.A. Bautista

**Table 1.** Target terms and energies for Ni II

Term		E <sup>a</sup> (observed)	E(present)	E(NS)
$3d^9$	$^2D$	0.0000	0.0	0.0
$3d^8(^3F)4s$	$^4F$	0.0798	0.0740	0.0314
$3d^8(^3F)4s$	$^2F$	0.1236	0.1234	0.0776
$3d^8(^3P)4s$	$^4P$	0.2128	0.2556	0.2114
$3d^8(^1D)4s$	$^2D$	0.2181	0.2439	0.1985
$3d^8(^3P)4s$	$^2P$	0.2610	0.3065	0.2605
$3d^8(^1G)4s$	$^2G$	0.2908	0.3283	0.2824

<sup>a</sup>Sugar & Corliss (1985)

$\lambda 7155$ , which could not be analyzed using the dataset by PZ and ZP.

Reliable ab initio calculations of atomic processes require first of all the computation of target wave functions that represent accurately the ionic systems. However, for complex ions such as Ni II and Fe II the target representations involve the inclusion of large numbers of correlation configurations and, as a consequence, very large close-coupling expansions that become computationally intractable even on supercomputers. New possibilities towards the computation of these very large atomic systems, and ab-initio calculations in general, are afforded by the new technology of massively parallel processors (MPP's). The present work reports new calculations, using the R-matrix method, carried out on the MPP CRAY T3D. The Iron Project R-matrix package of codes (Hummer et al. 1993) was adapted for this work to the massively parallel environment including up to 32 processors. The calculations presented here are limited to the low lying even parity terms that yield some of the most important IR and Optical lines. In the next section, we describe the atomic calculations and present the results for the collision strengths. Section 3 is devoted to the calculation of Maxwellian averaged collision strengths and the comparison of these values with earlier data. In Sect. 4, we discuss the excitation rates as well as some line emissivity ratios. Section 5 describes briefly the parallelization of the R-matrix calculations. Finally, in Sect. 6 we present discussion and conclusions.

## 2. Atomic calculations

### 21. Target data

The 7-term LS expansion for Ni II is a subset of a larger wave functions representation of the ion that includes the lowest 30 even and odd parity terms, i.e. all the levels up to 0.7224 Rydberg above the ground state. This larger representation of the target is dominated by the configurations  $3d^9$ ,  $3d^8 4s$ ,  $3d^8 4p$  and  $3d^7 4s^2$ ; however, the 7-term LS expansion used in this calculation is dominated by the configurations  $3d^9$  and  $3d^8 4s$  only. We have optimized the target expansion over all the configurations, for configuration interaction as well as for future work involving the odd parity levels. In Table 1 we present the calculated and the observed target term energies for the terms relevant to the present calculation averaged over the fine structure. The observed energies are taken from Sugar & Corliss (1985). The earlier target energies obtained by NS are also given and it is seen that the present ones are in much better agreement with the observed values, within about 5–10%. Another indication of the accuracy of the target wave function is the reasonably good agreement obtained ( $\sim 10 - 30\%$ ) between calculated length and velocity  $f$ -values, as shown in Table 2.

For Fe II we use a subset of an accurate and more extensive target wave function representation (52 LS terms) that is being used to compute radiative data, photoionization cross sections and transition probabilities for Fe I (Bautista & Pradhan 1995b; Bautista 1995). The expansion considered for the present calculation consists of the lowest 18 LS terms. Table 3 gives the target symmetries included and their calculated energies, compared with those obtained by Pradhan & Berrington (1993). The present target energies compare better with the experimental values. The calculated length and velocity  $f$ -values also show good agreement with each other, and also with the observed values (Fuhr et al. 1988) and the theoretical values by Nahar (1995) calculated for the Opacity Project. The present  $f$ -values seem to agree better with the observed values than those by Pradhan & Berrington (1993), as shown in Table 4.

### 22. Collision strengths: Calculations

It has been shown by ZP that the relativistic effects are not significant for the low-lying fine structure transitions in ions such as Fe II and Fe III. We therefore carried out non-relativistic calculations of the scattering matrixes in the LS coupling scheme. The fine structure collision strengths were obtained by an algebraic transformation of the scattering matrixes to the pair coupling scheme using a parallelized version of the code STGFJ. Partial wave contributions are included from total angular momenta  $J = 0 - 9$  for the case of Ni<sup>+</sup>, and  $J = 0 - 14$  for Fe<sup>+</sup>. We considered

**Table 2.** Sample of oscillator strengths for Ni II

Transition	$gf_i$	$gf_v$
$a^2D - z^2F^o$	0.70267	0.59782
$a^2D - z^2D^o$	1.59759	1.28159
$a^2D - y^2F^o$	0.49559	0.40461
$a^2D - z^2P^o$	0.37276	0.26010
$a^4F - z^4D^o$	5.41323	3.86574
$a^4F - z^4G^o$	10.4175	15.7351
$a^4F - z^4F^o$	7.75346	7.76380
$a^2F - z^2G^o$	4.60849	7.93458
$a^2F - z^2F^o$	3.63620	4.31824
$a^2F - z^2D^o$	2.61489	2.39635
$a^2F - y^2D^o$	0.10583	0.11570
$b^2D - z^2F^o$	0.00319	0.00157
$b^2D - z^2D^o$	0.04774	0.04222
$b^2D - y^2D^o$	2.74048	2.97062
$b^2D - z^2P^o$	3.59285	5.18373
$a^4P - z^4D^o$	0.11126	0.23252
$a^4P - z^4P^o$	3.34886	3.38832
$a^2P - z^2P^o$	0.25738	0.29348

**Table 3.** Target terms and energies for Fe II

Term	$E^a(\text{observed})$	$E(\text{present})$	$E^b(\text{PB})$
$3d^6(^5D)4s$	$a^6D$	0.0	0.0
$3d^7$	$a^4F$	0.0186	0.0182
$3d^6(^5D)4s$	$a^4D$	0.0953	0.0720
$3d^7$	$a^4P$	0.1302	0.1203
$3d^7$	$a^2G$	0.1604	0.1427
$3d^7$	$a^2P$	0.1737	0.1651
$3d^7$	$a^2H$	0.2146	0.1835
$3d^7$	$a^2D$	0.1934	0.1861
$3d^6(^3P)4s$	$b^4P$	0.2303	0.1914
$3d^6(^3H)4s$	$a^4H$	0.2242	0.1918
$3d^6(^3F)4s$	$b^4F$	0.2452	0.2040
$3d^54s^2$	$a^6S$	0.2461	0.2087
$3d^6(^3G)4s$	$a^4G$	0.2761	0.2310
$3d^6(^3P)4s$	$b^2P$	0.2861	0.2347
$3d^6(^3H)4s$	$b^2H$	0.2808	0.2354
$3d^6(^3F)4s$	$a^2F$	0.2663	0.2463
$3d^6(^3G)4s$	$b^2G$	0.3330	0.2746
$3d^6(^3D)4s$	$b^4D$	0.3480	0.2825

88  $SL\pi$  symmetries (that denote the total spin, angular momenta, and parity of the e-ion system) for Ni II with

$$L \leq 10$$

$$(2S + 1) = 1, 3, 5, 7$$

$$\pi = \text{even and odd}$$

The Fe II calculations included 128  $SL\pi$  symmetries with

$$L \leq 15$$

$$(2S + 1) = 1, 3, 5, 7$$

$$\pi = \text{even and odd.}$$

The collision strengths for both Ni II and Fe II were calculated for over 1000 energies ranging from 0 to 1 Rydberg. The energy mesh was chosen carefully as to ensure that the resonance structures, particularly near the excitation thresholds, are resolved well enough to calculate accurate Maxwellian averaged rate coefficients.

<sup>a</sup> Sugar & Corliss (1985)

<sup>b</sup> Pradhan & Berrington (1993)

### 23. Collision strengths: Results

In this section we compare our results with those by NS, and PZ and ZP, for Ni II and Fe II respectively. We find that although NS did not calculate collision strengths as a function of electron energy for Ni II, their single point values for the strongest transitions appear to approximate the average of our results. For weaker transitions however (smaller collision strengths), their values differ significantly from our results owing to the coupling and the resonance effects not included in their calculation. Figures 1a and b show the present collision strengths for Ni II, along with the single collision strength calculated by NS, for some of the stronger transitions, with good agreement with one of them and up to about 40% difference with

**Table 4.** Sample of oscillator strengths for Fe II

Transition	$gf_i$	$gf_v$	$gf_i(\text{PB})$	$gf_v(\text{PB})$	$gf^a(\text{obs.})$	$gf^b(\text{N95})$
$a\ ^6D - z\ ^6D^\circ$	9.18	8.60	10.2	9.9	9.86	7.76
$a\ ^6D - z\ ^6F^\circ$	12.86	14.36	14.4	14.1	14.3	11.3
$a\ ^6D - z\ ^6P^\circ$	5.01	5.11	6.3	6.0	6.19	3.87
$a\ ^4F - z\ ^4D^\circ$	2.04	0.80			2.05	1.37
$a\ ^4F - z\ ^4F^\circ$	1.02	0.39			1.04	0.87
$a\ ^4D - z\ ^4D^\circ$	4.74	7.34	5.8	7.6	6.67	4.36
$a\ ^4D - z\ ^4F^\circ$	6.65	11.93	8.2	10.8	9.23	6.61
$a\ ^4D - z\ ^4P^\circ$	2.87	4.46	3.8	4.2	4.11	2.63
$a\ ^4P - z\ ^4D^\circ$	0.27	0.16			0.30	0.20
$a\ ^4P - z\ ^4P^\circ$	0.85	0.44			0.97	0.79

<sup>a</sup> Fuhr et al. (1988)<sup>b</sup> Nahar (1995)

the other. It is noted that the presence of resonance structures in the present collision strengths would enhance the Maxwellian averaged values, although the resonances appear to be weak.

Comparing the present collision strengths for Fe II with those by PZ and ZP we find that in general the background of the collision strengths in both sets of data are similar and the differences are mostly in the positions and strength of the resonances.

Figure 2 compares our results for the  $^6D_{9/2} - ^6D_{7/2}$  transition in Fe II with the results by PZ. It is noticed that both calculations give very similar background for the cross sections; however there are differences in the structure of the resonances.

We expect the present results to be more accurate than those by ZP because of our better representation of the target. One exception may be the region above 0.22 Rydberg where ZP obtain a complex of resonances due to the coupling to odd parity levels in Fe II that are not included in the present computation. However for the forbidden transitions of interest, these high lying resonances are not expected to affect significantly the Maxwellian averaged values for temperatures below 50,000 K.

### 3. Rate coefficients

Maxwellian averaged effective collision strengths are given by

$$\Upsilon_{ij} = \int_0^\infty \Omega_{ij} e^{-E_j/kT} d(-E_j/kT) \quad (1)$$

Here,  $\Omega_{ij}$  is the collision strength corresponding to the transition from level  $i$  to level  $j$ ,  $E_j$  is the energy of the incident electron with respect to the excitation threshold of the level  $j$ , and  $T$  is the temperature.

In Tables 5 and 6 we present samples of our results for Maxwellian averaged collision strengths at 10,000 K for Ni II and Fe II, and compare them with previous results by NS and PZ respectively. Our results agree well (10–20%) with the single point collision strengths by Nussbaumer & Storey (1982) for the transitions that give rise to some of the strongest lines, e.g.  $^2D_{5/2} - ^2F_{7/2}$ . However, for other transitions the differences range from 30% to more than a factor of two. When comparing our results with those by PZ and ZP, the overall difference is about 30%, being systematically smaller for the stronger transitions and greater for the weaker ones. These differences in Fe II are due likely to more accurate target representation and resonance structures in the present work. Nonetheless, the overall differences between the present calculations and that by PZ and ZP are within their stated uncertainty for the transitions considered herein,  $\approx 30\%$ .

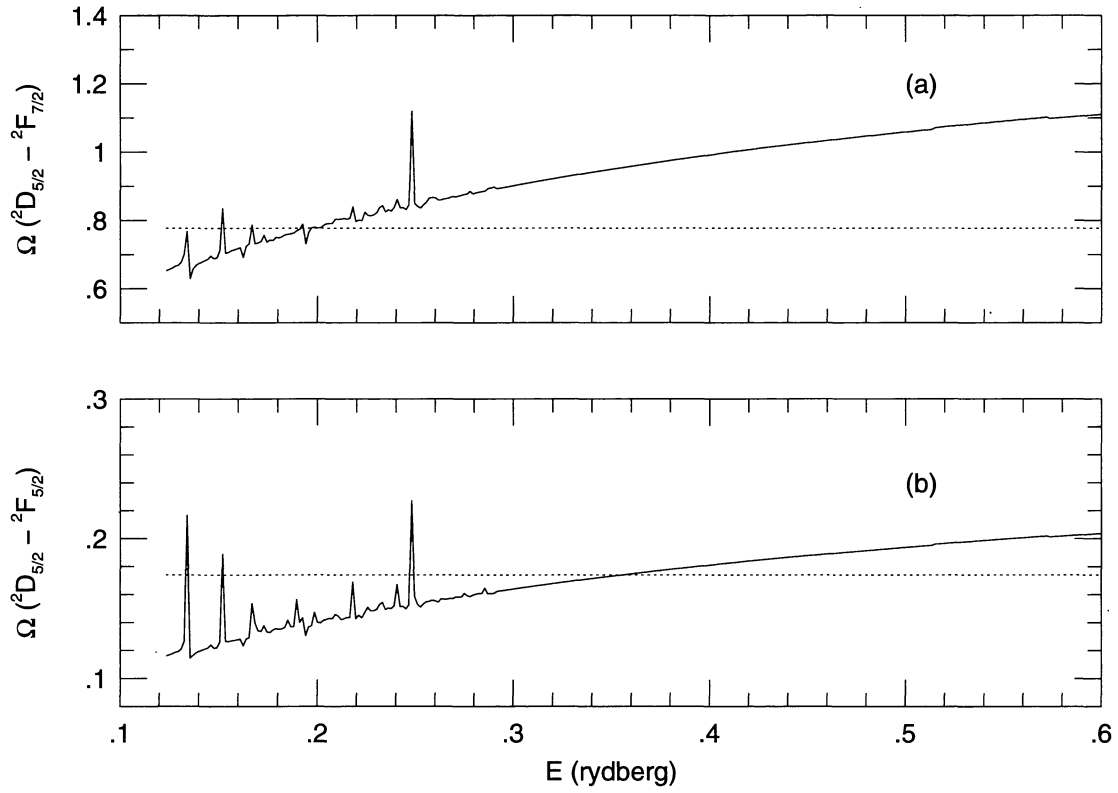


Fig. 1. Excitation collision strengths for the transitions ( ${}^2D_{5/2} - {}^2F_{7/2}$ ) a) and ( ${}^2D_{5/2} - {}^2F_{5/2}$ ) b) in Ni II vs. incident energy. The dashed lines indicate the one point values by NS

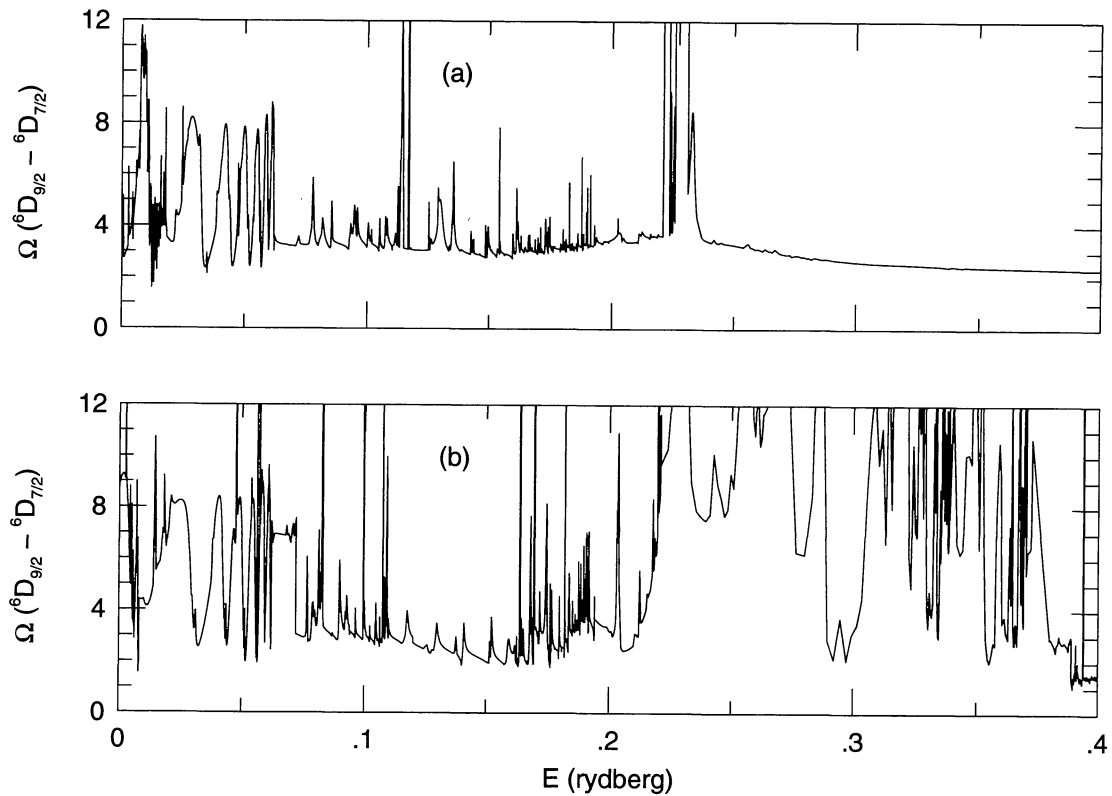


Fig. 2. Collision strengths for the transition ( ${}^6D_{9/2} - {}^6D_{7/2}$ ) in Fe II from present computation a) and PZ b)

**Table 5.** Comparison of Maxwellian averaged collision strengths for Ni II

Transition	$\Upsilon(10^4 K)$ [present]	$\Upsilon(10^4 K)$ [NS]
$^2D_{5/2} - ^2D_{3/2}$	0.113	0.148
$^2D_{5/2} - ^4F_{9/2}$	0.165	0.230
$^2D_{5/2} - ^4F_{7/2}$	0.088	0.144
$^2D_{5/2} - ^4F_{5/2}$	0.041	0.062
$^2D_{5/2} - ^4F_{3/2}$	0.015	0.024
$^2D_{5/2} - ^2F_{7/2}$	0.749	0.777
$^2D_{5/2} - ^2F_{5/2}$	0.135	0.174
$^2D_{5/2} - ^4P_{5/2}$	0.042	0.088
$^2D_{5/2} - ^4P_{3/2}$	0.021	0.049
$^2D_{5/2} - ^4P_{1/2}$	0.009	0.022
$^2D_{5/2} - b \ ^2D_{3/2}$	0.046	0.167
$^2D_{5/2} - b \ ^2D_{5/2}$	0.140	0.095
$^2D_{5/2} - ^2P_{3/2}$	0.184	0.132
$^2D_{5/2} - ^2P_{1/2}$	0.054	0.049
$^2D_{5/2} - ^2G_{9/2}$	0.184	0.215
$^2D_{5/2} - ^2G_{7/2}$	0.050	0.114

Effective collision strengths are obtained for all the transitions calculated in this work for temperatures ranging from 500 K to 50,000 K. For brevity we do not give the complete set of data in this paper, but it is available electronically via Internet by request to the authors.

#### 4. Diagnostic line ratios

Given the importance of using [Fe II] and [Ni II] lines as diagnostics of density and temperature in plasmas, we have calculated some prominent line emissivity ratios as functions of the electron density,  $N_e$ , and the temperature,  $T_e$ . For Ni II we have taken the  $A$ -values reported by NS and for Fe II we use  $A$ -values by Nussbaumer & Storey (1988) for the IR lines, and  $A$ -values by Garstang (1962) for the remaining transitions.

Figures 3a and b show two different emissivity line ratios for Ni II calculated with the present data (solid lines), and with that by NS (dashed line). We find that at least for emissivity ratios between the stronger [Ni II] lines our results agree with those ratios by NS to within about

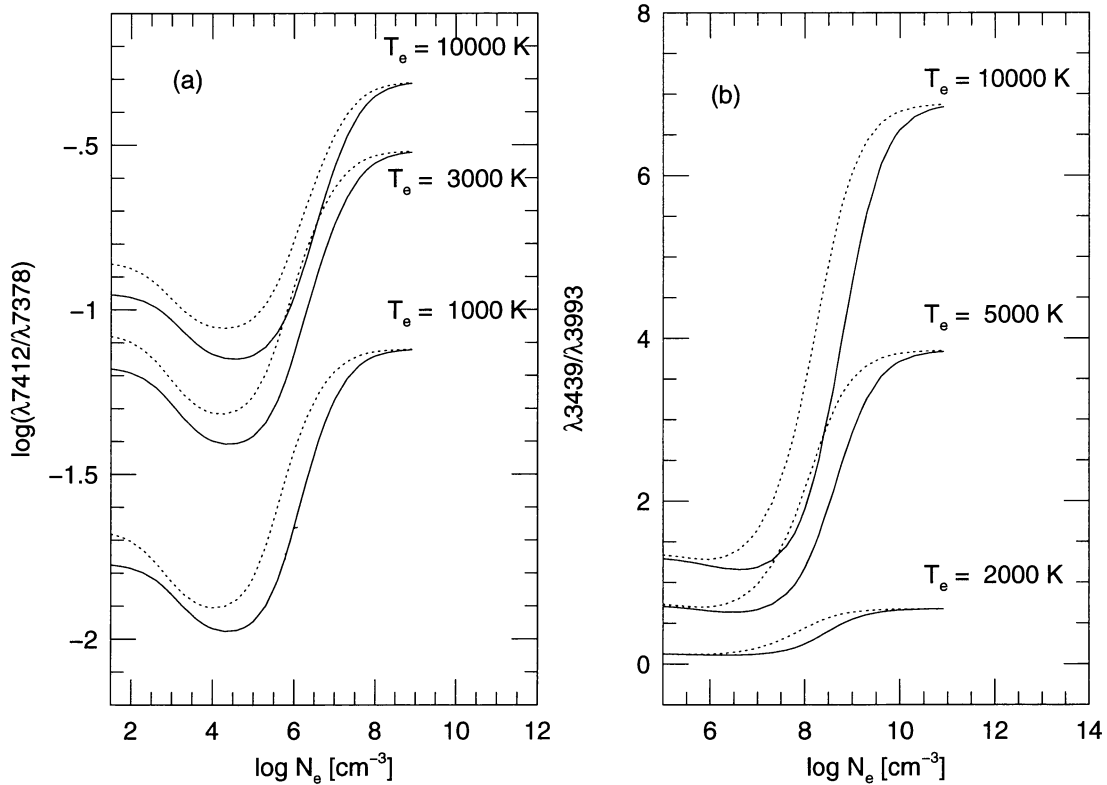
0.4 dex in  $N_e$ . Nonetheless, even if the emissivity ratios agree reasonable well for these transitions, our individual excitation rates overall may be quite different from those by NS, and that is expected to affect the derived abundances of Ni II in astrophysical sources (work in progress).

The emissivity ratios calculated from the present data are compared with those using the PZ and ZP data in Figs. 4a-d. In many cases the agreement is very good as seen in Fig. 4a. However, some line ratios vary by up to 0.6 dex in  $N_e$  (see Figs. 4b and c). It is particularly noted that the present line ratios confirm the diagnostics obtained with the PZ and ZP data of the inferred presence on high density regions,  $N_e \approx 10^6 \text{ cm}^{-3}$ , in partially ionized zones in Orion (Bautista et al. 1994; Bautista & Pradhan 1995), as well as the diagnostics of [Fe II] IR lines from late time spectra of SN1987A (Bautista et al. 1995).

Line emissivities and emissivity ratios for various temperatures and electron densities can be obtained from the authors.

**Table 6.** Comparison of Maxwellian averaged collision strengths for Fe II

Transition	$\Upsilon(10^4 K)$ [Present]	$\Upsilon(10^4 K)$ [PZ]
${}^6D_{9/2} - {}^6D_{7/2}$	4.65	5.52
${}^6D_{9/2} - {}^6D_{5/2}$	1.29	1.49
${}^6D_{9/2} - {}^6D_{3/2}$	0.813	0.675
${}^6D_{9/2} - {}^6D_{1/2}$	0.433	0.284
${}^6D_{9/2} - {}^4F_{9/2}$	1.31	3.60
${}^6D_{9/2} - {}^4F_{7/2}$	0.614	1.51
${}^6D_{9/2} - {}^4F_{5/2}$	0.135	0.497
${}^6D_{9/2} - {}^4F_{3/2}$	0.016	0.137
${}^6D_{9/2} - {}^4D_{7/2}$	14.3	11.0
${}^6D_{9/2} - {}^4D_{5/2}$	0.572	0.560
${}^6D_{9/2} - {}^4D_{3/2}$	0.386	0.191
${}^6D_{9/2} - {}^4D_{1/2}$	0.233	0.061

**Fig. 3.** Emissivity line ratios for Ni II as function of electron density for different temperatures calculated from present collision strengths (solid lines), and from those by NS (dashed lines)

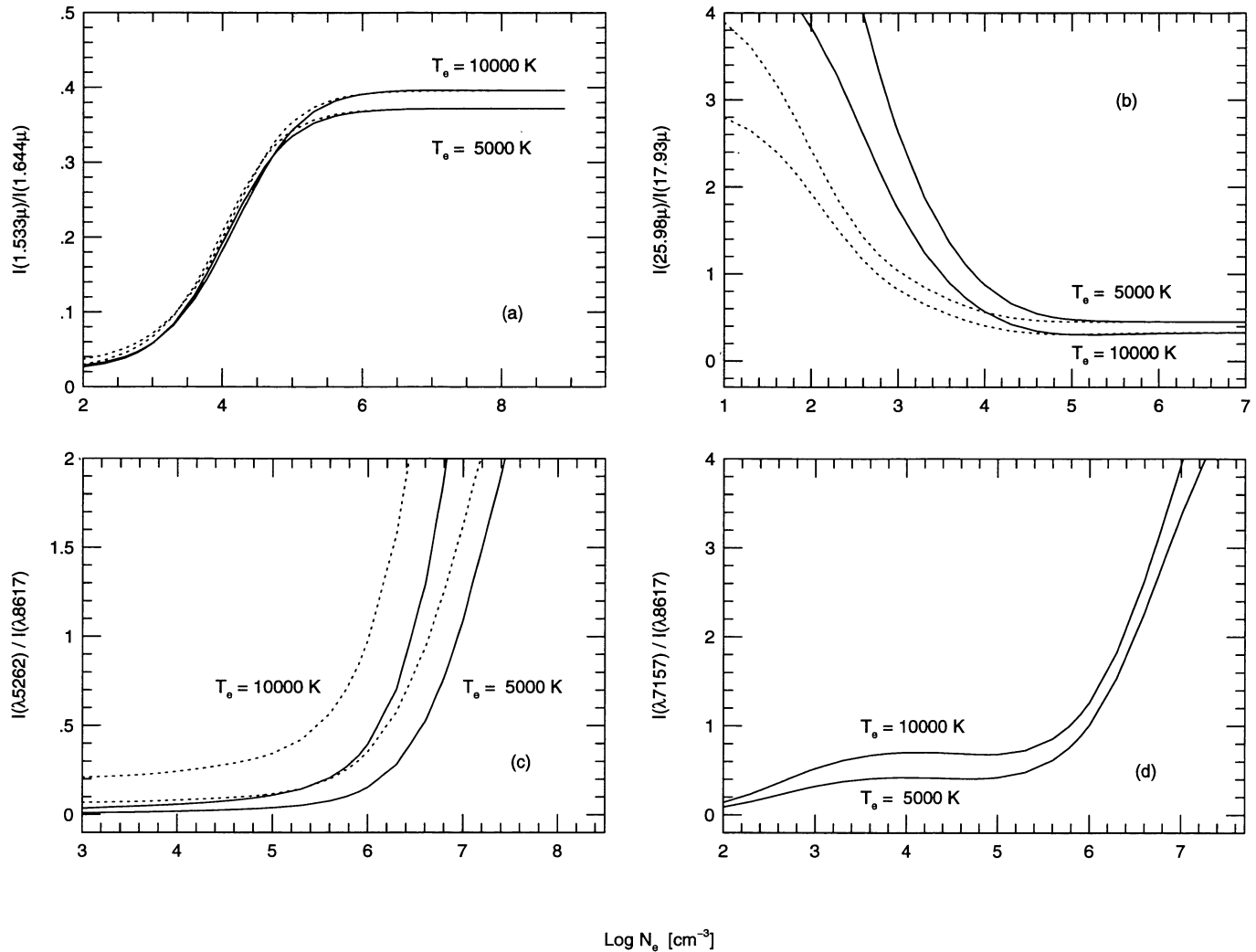


**Fig. 4.** Emissivity line ratios for Fe II as function of electron density for different temperatures calculated from present collision strengths (solid lines), and from those by PZ and ZP (dashed lines). The transitions corresponding to the emissivity ratio in panel (d) are not included in the PZ and ZP calculations

## 5. Massively parallel R-matrix computations

The present calculations were carried out using a newly adapted version of the R-matrix codes on the MPP Cray T3D, using up to 32 parallel processors. The computations are parallelized primarily according to the total spin and angular symmetries,  $SL\pi$ , in the inner region R-matrix codes STG1, STG2, and STGH, and incident electron energies in the asymptotic codes such as STGF and its fine structure version STGFJ. Speed-ups of the codes are nearly linear with the number of processors and reach up to a factor of ten over serial processing on the Cray Y-MP. Also, by shearing the largest arrays in the codes among the multiple processors we can expand the RAM memory up to nearly 250 Mega words. The parallelization on MPP's affords new opportunities for ab initio computa-

tions, particularly using the R-matrix method for atomic processes.

## 6. Conclusion

Collisional excitation rates and emissivity ratios for Ni II and Fe II are reported. It is found that the present collision strengths for Ni II differ considerably for some transitions from those reported by NS. However, for the strongest transitions, which give rise to some of the observable lines in nebular spectra, the agreement between both sets of data is reasonably good. This suggests, in particular, that the accuracy of the atomic data may not be responsible for the longstanding nickel-to-iron abundance problem as suggested by Henry & Fesen (1988). Recently, it has been proposed that [Ni II] lines may be excited by continuum fluorescence (Lucy 1995). A detailed study of this and



other excitation mechanisms is presented in Bautista et al. (1996).

The data presented here for Fe II complements the set of transitions computed by PZ and ZP, by including the doublet and sextet states that were excluded from their computations. The typical difference between the present results for Fe II and those by PZ and ZP is within the uncertainty stated by those authors, about 30%. Fe II data for the transitions considered in the present work should be somewhat more accurate, < 20%. The calculated emissivity ratios from both sets of data also agree reasonably well and confirm much of the [Fe II] line diagnostics recently reported for different astronomical objects. However, it should be noted that for some weak transitions the present results do differ considerably from the earlier works.

*Acknowledgements.* We are grateful to the staff at the Ohio Supercomputer Center in Columbus Ohio for their help with the new CRAY T3D. We would like to thank Dr. Hong Lin Zhang for assistance with some calculations. This work was supported in part by the U.S. National Science Foundation (PHY-9421898) grant for the Iron Project.

## References

- Bautista M.A., 1995, A&AS (submitted)  
 Bautista M.A., Pradhan A.K., 1995a, ApJ 462, L65  
 Bautista M.A., Pradhan A.K. 1995b, J. Phys. B Lett. 28, L173  
 Bautista M.A., DePoy D.L., Pradhan A.K., et al., 1995, AJ 109, 729  
 Bautista M.A., Peng J., Pradhan A.K., 1996, ApJ (in press)  
 Bautista M.A., Pradhan A.K., Osterbrock D.E., 1994, ApJ 432, L135  
 Dennefeld M., 1986, A&A 157, 267  
 Dennefeld M., Péquignot D., 1983, A&A 127, 42  
 Fuhr J.R., Martin G.A., Wiese W.L., 1988, J. Phys. Chem. Ref. Data 17, Suppl. 4  
 Garstang R.H., 1962, MNRAS 124, 321  
 Grandi S.A., 1975, ApJ 199, L43  
 Henry R.B.C., Fesen R.A., 1988, ApJ 329, 693  
 Henry R.B.C., MacAlpine G.M., Kirshner R.P., 1984, ApJ 278, 619  
 Hudgins D., Herter T., Joyce R.J., ApJ 354, L57  
 Hummer D.G., Berrington K.A., Eissner W., et al., 1993, A&A 279, 298  
 Johnson D.R.H., Barlow M. J., Drew J.E., Brinks E., 1992, MNRAS 255, 261  
 Lucy L.B., 1995, A&A 294, 555  
 Nahar S.N., 1995, A&A 293, 967  
 Nussbaumer H., Storey P., 1982, A&A 110, 295  
 Nussbaumer H., Storey P., 1988, A&A 193, 327  
 Osterbrock D.E., Tran H.D., Veilleux S., 1992, ApJ 389, 305  
 Pradhan A.K., Berrington K.A., 1993, J. Phys. B 26, 157  
 Pradhan A.K., Zhang H.L., 1993, ApJ 409, L77  
 Rudy R.J., Rossano G.S., Puetter R.C., 1994, ApJ 426, 646  
 Sugar J., Corliss C., 1985, J. Phys. Chem. Ref. Data 14, Suppl. 2  
 Stahl O., Wolf B., 1986, A&A 158, 371  
 Zhang H.L., Pradhan A.K., 1995, A&A 293, 953